

# Equilibrium Phase Diagrams

## CHAPTER PREVIEW

Most ceramics are multicomponent materials and the most stable phase at any temperature will be the one with the lowest free energy,  $G$ . One use of phase diagrams is to represent the phase or phases we might expect to be present as a function of temperature. There are a large number of books just concerned with this one topic. Much work was carried out in the 1950s and 1960s, but many systems have remained almost completely unexplored and it is not a well-funded area in the United States now. The lack of effort is in spite of the demonstration that new complex ceramics, such as the high-temperature superconductors YBCO and BiSCCO and the magnetic manganates, possess extraordinary, and potentially very useful, properties.

Much of the classical work on phase equilibria has actually been concerned with processing metals. Thus the Fe–O phase diagram is perhaps the most thoroughly characterized because of its importance to the iron and steel industry.

A word to keep in mind throughout our discussion is equilibrium: we are talking about equilibrium phase diagrams. Often we use a phase diagram as a guide to processing. If the process is in progress then it is not in equilibrium. And, by definition, a chemical reaction is not an equilibrium process. If a reaction is exothermic then a rise in temperature favors the reactants. Although most of the phase diagrams we use in ceramics are for a pressure of 1 atmosphere, in one-component systems such as carbon, pressure is a very important variable. It tells us what pressure we need for direct synthesis of diamond. In metal–oxygen diagrams the partial pressure of oxygen determines what is the stable form of the oxide.

## 8.1 WHAT'S SPECIAL ABOUT CERAMICS?

Since many ceramics are oxides, the oxygen partial pressure,  $pO_2$ , is an important variable. There is a lot of information about many metal–oxygen systems. In part, this is due to interest in how to obtain metals by direct reduction from their oxides. A frequent way of representing free energies of formation of oxides as a function of  $pO_2$  and  $T$  is the Ellingham diagram (Ellingham, 1944) that was popularized by Richardson and Jeffes (1948) for iron and steel production. Much less is known about nitrides and oxynitrides or even carbides.

Many ceramics are multicomponent materials and, hence, many of the important phase diagrams involve three or more components. Here are some

examples of where phase diagrams have very practical applications in the use of ceramics:

**Refractory silica brick:** This was used for the roof of the open-hearth furnace, which was once an important method for steel production. Now silica refractories are used in coke ovens and as roofs in glass tanks. Typical operating temperatures are 1625–1650°C. The phase diagram tells us that the  $SiO_2$  needs to be quite pure (only 0.2–1.0 wt%  $Al_2O_3$ ) or it will melt.

**Fire-clay brick:** This is a classic clay product with composition close to kaolinite. Although it is used at temperatures below 1587°C, the phase diagram tells us that some liquid will often be present since these ceramics contain 22–33 wt%  $Al_2O_3$ . This material is so important because it performs the task very well and is cheap to produce.

### DALTON'S LAW OF PARTIAL PRESSURES

$$P_A = X_A P$$

$P_A$  is the partial pressure of A.  
 $X_A$  is the mole fraction of A.  
 $P$  is the total pressure of the gas mixture.

Barium titanate: Pure cubic BaTiO<sub>3</sub> single crystals cannot be grown from a melt of that composition because the hexagonal phase is in equilibrium with the liquid at the solidification temperature (1618°C). Although the hexagonal phase is transformed to the cubic phase at 1460°C, the phase change is sluggish and thus the hexagonal phase can exist at room temperature. The hexagonal form of BaTiO<sub>3</sub> is not ferroelectric, which is the property in which we are most often interested. In Chapter 29 we describe how single crystals of cubic BaTiO<sub>3</sub> can be grown.

Adhesion of metals in integrated circuits: Aluminum has been used for over 30 years as interconnect and top-level metallization in integrated circuits. One of the reasons Al is so good is that it reduces SiO<sub>2</sub> to form interfacial metal–oxide bonds that promote adhesion and stability. One of the problems with copper metallizations is that SiO<sub>2</sub> is more stable than Cu<sub>2</sub>O. Despite this difficulty, Cu has several significant advantages over Al and is now used in many commercial devices such as IBM’s processor for the Apple G5, Intel’s Pentium IV, and AMD’s Athlon. The relative oxidizing powers of metals are represented frequently on Ellingham diagrams. In Chapter 15 we will show how these diagrams can be useful in developing brazes for ceramics.

## 8.2 DETERMINING PHASE DIAGRAMS

We refer you to basic thermodynamics texts for the details on the origin of phase diagrams and the phase equilibria book by Bergeron and Risbud. In this section we will just summarize some key points. First, some thermodynamic background to phase diagrams is presented.

- The phase with the lowest free energy,  $G$ , is thermodynamically stable.
- The chemical potential,  $\mu_i$ , of a component is the same in all of the phases in which it is present. This requirement is used in the derivation of Gibbs Phase Rule.
- At equilibrium the temperatures and pressures of all phases are equal.

Determining a phase diagram requires measuring which phases are in equilibrium under well-defined conditions. An especially critical factor for ceramics is being sure that we have equilibrium. In ceramics we have two challenges:

- We need to make measurements at high temperature where direct determination of phases is difficult.
- The valence of the cations may change as the temperature or pressure changes. If the cation is polyvalent, then the valence depends on the oxygen activity, which, as we will see later, depends on the partial pressure of oxygen,  $pO_2$ .

To ensure we have equilibrium, the two bulk phases should really be in intimate contact separated by a flat (planar) interphase boundary.

The number of techniques we can use for direct determination of phase diagrams of ceramic systems is quite limited because of the requirements for high temperatures.

- High-temperature X-ray diffraction. The maximum operating temperatures are up to 2500°C in high vacuum, 2400°C in inert atmospheres, and 1700°C in air.
- TEM with hot-stage. The maximum temperature is usually 1300°C, working in vacuum, typically  $\sim 10^{-4}$  Pa, so there is no control of  $pO_2$ .

Most techniques that are used to determine phase diagrams experimentally use an indirect approach. Note that often we are not trying to determine an entire diagram, but rather the specific parts that may be of interest, such as the solvus lines, the liquidus, or the eutectic temperature. Figure 8.1 shows an example of using cooling curves to determine the liquidus and eutectic temperature for a binary system. Heating curves produce similar results and are often easier to achieve experimentally. Phase changes produce the deviations in the time–temperature curves. These measurements would be made using differential

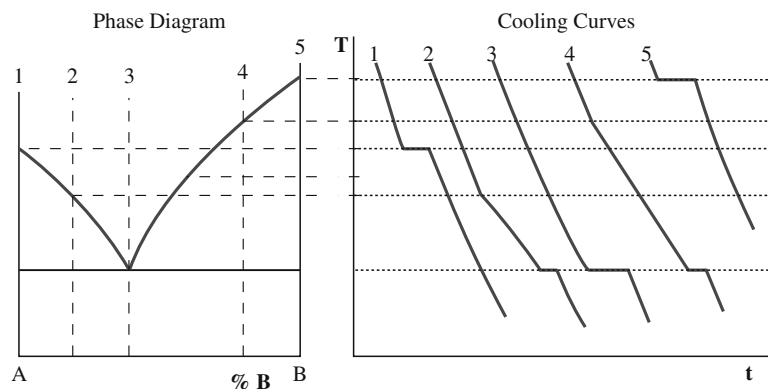


**FIGURE 8.1** Illustration of the use of cooling curves to determine the liquidus and eutectic in a binary phase diagram.

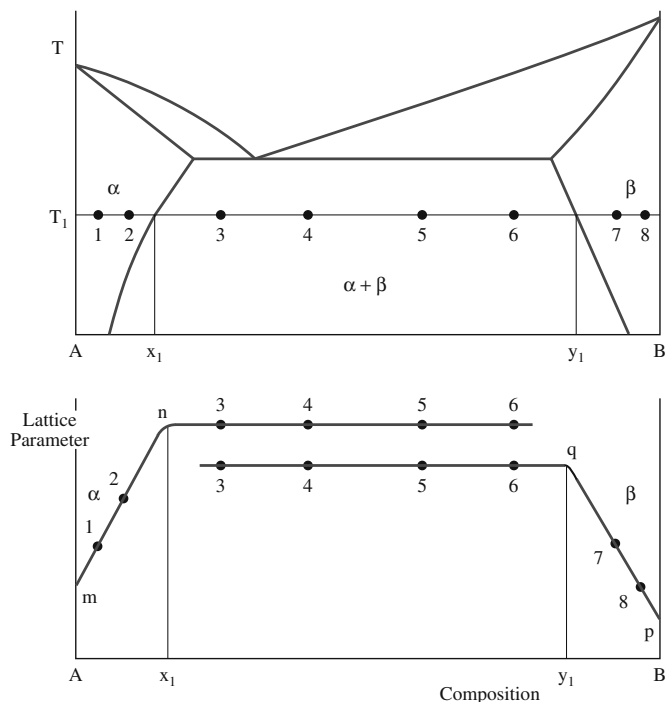


**FIGURE 8.2** Parametric method for determination of the solvus lines in a binary phase diagram.

thermal analysis (DTA) or differential scanning calorimetry (DSC). Maximum temperatures for these instruments are about 1700°C. At this temperature many of the important ceramics such as Al<sub>2</sub>O<sub>3</sub> (melts at 2054°C), SiO<sub>2</sub> (melts at 1710°C), and ZrO<sub>2</sub> (melts at 2677°C) are still solid. Another problem with ceramic melts, especially those containing SiO<sub>2</sub>, is their high viscosity. Most oxide glasses are silicates. Crystallization from these melts is often difficult and reaching equilibrium can take a very long time (years!).

A frequently used method for studying phase equilibria in ceramics is X-ray diffraction on samples that have been equilibrated at high temperature then quenched. This technique is particularly useful for the solid-state portions of the phase diagram, such as determining the position of the solvus lines. In each single solid-solution region of a binary phase diagram there is a change in lattice parameter with composition. In the phase field where both solid solutions exist the lattice parameter of each solid solution remains constant with composition as shown in Figure 8.2. The position of the solvus line,

**CLAUSIUS–CLAPEYRON EQUATION**

Change in vapor pressure (*P*) of a solid with a change in *T*

$$\frac{dP}{dT} = \frac{\Delta H_s}{T(V_v - V_s)}$$

$\Delta H_s$  = enthalpy of sublimation of solid  
 $V_v$  = molar volume of vapor  
 $V_s$  = molar volume of solid

**SOME USEFUL DATA**

NiO  $T_M = 2257$  K;  $\Delta H_f = 50.6$  kJ/mol  
MgO  $T_M = 3073$  K;  $\Delta H_f = 77.4$  kJ/mol  
BeO  $T_M = 2830$  K;  $\Delta H_f = 71.1$  kJ/mol  
UO<sub>2</sub>  $T_M = 3150$  K;  $\Delta H_f = 54.0$  kJ/mol

at a particular temperature, corresponds to the change in slope. It is important that the conditions are sufficient for the system to reach equilibrium and that high-purity powders are used.

We can calculate phase diagrams using the requirement that the lowest free energy state is the equilibrium one. If calculations are performed for a range of temperatures then the phase boundaries can be determined. Because we often do not know the absolute values for thermodynamic quantities, but changes in these, we use the following expression:

$$\Delta G = \Delta H - T\Delta S \quad (8.1)$$

$\Delta H$  and  $\Delta S$  can be determined at any temperature using the heat capacity,  $c_p$ :

$$\Delta H_{T_2} - \Delta H_{T_1} = \int_{T_1}^{T_2} \Delta c_p dT \quad (8.2)$$

and

$$\Delta S_{T_2} - \Delta S_{T_1} = \int_{T_1}^{T_2} \frac{\Delta c_p}{T} dT \quad (8.3)$$

The problem is that heat capacities are not known for many compounds. As a result, we often make assumptions that allow us to determine the part of the phase diagram that is important to us.

### Estimation of Liquidus and Eutectic Temperature

#### for a Binary System

We can estimate the position of the liquidus assuming that our mixture forms an ideal solution, hence it obeys Raoult's law. From the Clausius–Clapeyron equation with some integration and algebraic manipulation we can obtain

$$\ln X_A = -\frac{\Delta H_f}{R} \left( \frac{T_M - T}{T_M T} \right) \quad (8.4)$$

where  $X_A$  is the mole fraction of component A and  $\Delta H_f$  is the enthalpy of fusion. Values of  $T$  are plotted against composition. At the intersection of these lines is the eutectic point. This approach works well for many alkali halide systems (such as the NaF–KF) but

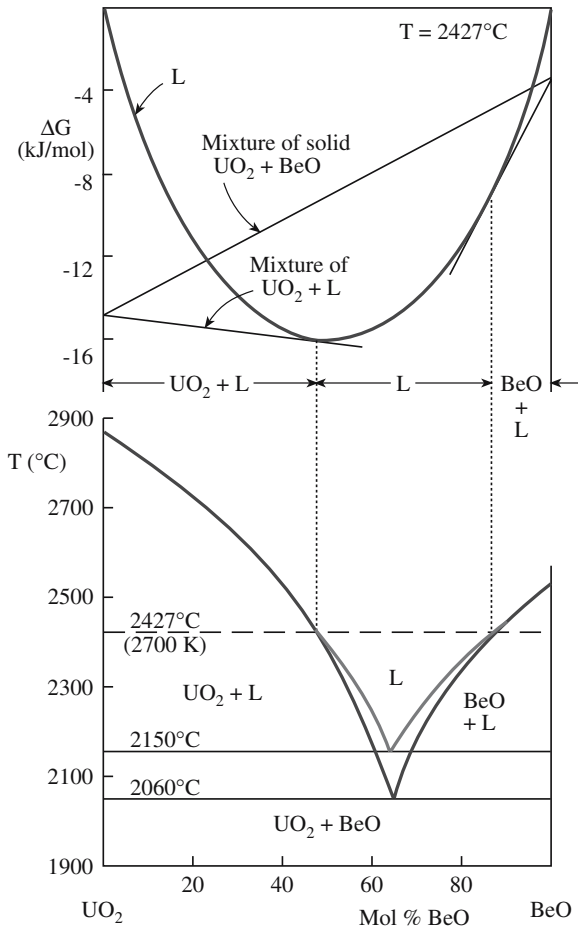


**FIGURE 8.3** The  $\text{UO}_2$ - $\text{BeO}$  phase diagram determined using free energy calculations.

not so well for many oxides. For example, the  $\text{PbO}$ - $\text{B}_2\text{O}_3$  system shows dissociation on melting.

An alternative method to calculate the liquidus is to calculate differences in free energy of the solid ( $G_s$ ) and liquid ( $G_l$ ) phases as a function of temperature:

$$G_s - G_l = -\Delta H_f \ln \frac{T_M}{T} \quad (8.5)$$

We need to know the enthalpy of fusion,  $\Delta H_f$ , and the melting temperature,  $T_M$ .

Figure 8.3 shows how this method has been used to construct the phase diagram for the  $\text{UO}_2$ - $\text{BeO}$  system. The agreement with the published diagram is quite good.

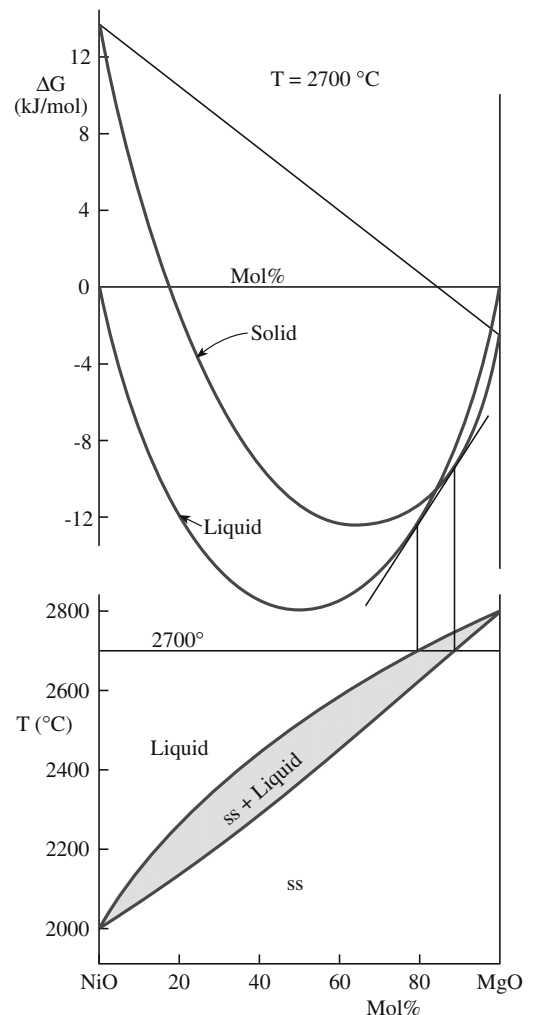
### Estimation of Liquidus and Solidus for Systems with Complete Solid Solubility

Figure 8.4 shows free energy versus composition plots at  $2700^\circ\text{C}$  for the  $\text{NiO}$ - $\text{MgO}$  system and the corresponding

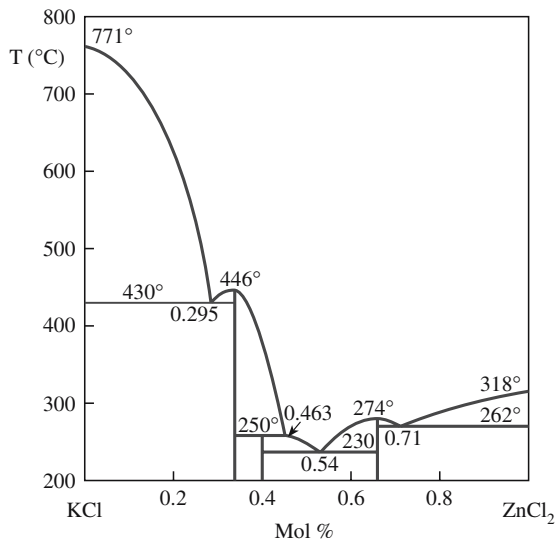
phase diagram. This system is one in which the components are mutually soluble in both the solid and liquid states. Determination of the free energy curves uses Eq. 8.5 and the free energy change associated with mixing liquid  $\text{NiO}$  and liquid  $\text{MgO}$ , which can be calculated using

$$\Delta G = RT[X \ln X + (1 - X) \ln(1 - X)] \quad (8.6)$$

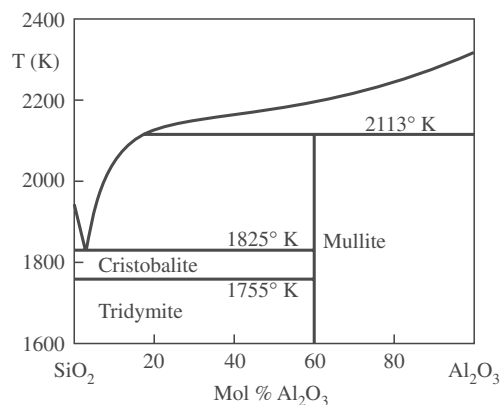
The use of computer methods for calculating phase diagrams is becoming increasingly important. The results of many of these studies are available in CALPHAD: Computer Coupling of Phase Diagrams and Thermochemistry (Saunders, 1998 and on-line). Figure 8.5 illustrates such computed phase diagrams.



**FIGURE 8.4** The  $\text{NiO}$ - $\text{MgO}$  phase diagram and free energy curves at  $T = 2700^\circ\text{C}$ .



(A)



(B)

FIGURE 8.5 (a) CALPHAD phase diagram for KCl–ZnCl<sub>2</sub>. (b) CALPHAD phase diagram for SiO<sub>2</sub>–Al<sub>2</sub>O<sub>3</sub>.

### 8.3 PHASE DIAGRAMS FOR CERAMISTS: THE BOOKS

Because the books are really important for ceramics we will emphasize them here rather than just at the end of the chapter: all ceramicists must be familiar with “the books.” The first volume of the series, *Phase Diagrams for Ceramists*, was published in 1964 and is in daily use. The series currently contains 12 volumes. The companion volume by Bergeron and Risbud is entitled *Introduction to Phase Equilibria in Ceramics* and should always sit on the same shelf. The books are unique in that the later volumes contain both new and

#### GIBBS C, F, AND X

C is for component  
F is for freedom  
X is for phase

updated diagrams, but the old diagrams found in the earlier volumes are still often quoted. Many of these diagrams resulted from research in the 1950s and 1960s, but there are many going back to 1915. The first diagram in the book (Fig. 1), produced in 1951, is for the system Al–Al<sub>2</sub>O<sub>3</sub> and shows the gaseous species over liquid Al<sub>2</sub>O<sub>3</sub> as a function of  $T$  and  $P$ . One of the earliest is for the AgNO<sub>3</sub>–NaNO<sub>3</sub> system that was devised in 1900 (Fig. 1040). Unfortunately, this field is not currently well supported. In our brief discussion in this chapter, we take the approach of “learn by example.”

A warning on units is necessary. Since many of the data were collected before the establishment of SI units, the plots contain combinations of weight percent, mole fraction, and mole percent, kbars and atm for pressure, but fortunately only °C (not °F for temperature).

### 8.4 GIBBS PHASE RULE

We derive the Gibbs Phase Rule in three steps.

Step 1. Consider the situation in which we have  $C$  components that exist in  $X$  phases. If Fe and O are the components, Fe and FeO would be examples of phases. So there are  $XC$  composition variables. Adding the two important external variables in ceramics,  $P$  (pressure) and  $T$ , gives  $XC + 2$  variables.

Start with  $XC + 2$

Step 2. If we described the composition of a phase in terms of the mole fraction of its components, then when we have described all but one of the mole fractions, the last one must be known because together the mole fractions all add up to unity. This happens for each of the  $X$  phases, so  $X$  of the variables are actually fixed.

Deduct  $X$

Step 3. In equilibrium, the chemical potential of a component must be the same in all the phases (otherwise it will not be equilibrium). If the concentration is fixed in one phase then the chemical potential is fixed in that phase. The chemical potential must then be fixed in all the phases since it is the same in all phases. Thus, if the concentration is known in one phase, then  $X - 1$  variables (the concentrations in the other phases) are automatically fixed (even though they are not necessarily the same—their chemical potential is the same). Since this is true for all  $C$  of the components,  $(X - 1)C$  variables are fixed (they are not independent variables).

Deduct  $(X - 1)C$

Hence the number of independent variables is given by

$$F = (XC + 2) - X - (X - 1)C$$

Rearranging gives us Gibbs Phase Rule

$$F + X = C + 2 \quad (8.7)$$

Note that many texts use  $P$  for the number of phases and  $V$  for the degree of freedom. We use  $F$  for (degrees of) freedom,  $P$ , an important variable, for pressure,  $V$  for volume, and  $X$  for the number of phases.

Most of the time we just examine different systems with up to three components ( $C = 1, 2, \text{ or } 3$ ). The difficulty sometimes is in counting the components. There are also four- and five-component diagrams in ceramics. We always have to be aware that the sample might contain nonequilibrium phases.

### 8.5 ONE COMPONENT ( $C = 1$ )

In each of these examples, we have one component, meaning that the chemical composition of the material does not vary. From the phase rule we have  $P$  and  $T$  as two variables, which is what we plot in each case. Using  $F + X = C + 2$ , for a one-phase region we can vary both  $P$  and  $T$ . For a two-phase region (the line), if we vary  $P$  then  $T$  is determined. For a three-phase region in a one-component system there are no variables.

Example 1: Water: One component (Figure 8.6).  $X$  takes its maximum value of 3 when  $F = 0$ . The three coexisting phases are then solid, liquid, and gas at point A, or the liquid and two solid phases at point B. Points A and B occur at unique combinations of temperature and pressure. Lines correspond to locations where two

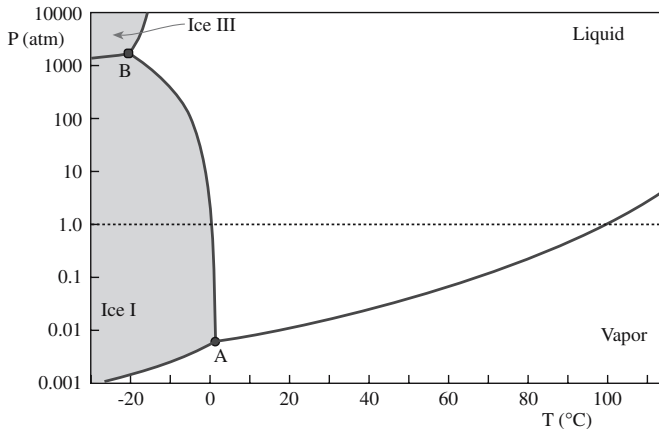


FIGURE 8.6 The  $\text{H}_2\text{O}$  phase diagram. (1000 atm is  $\sim 100$  MPa.)

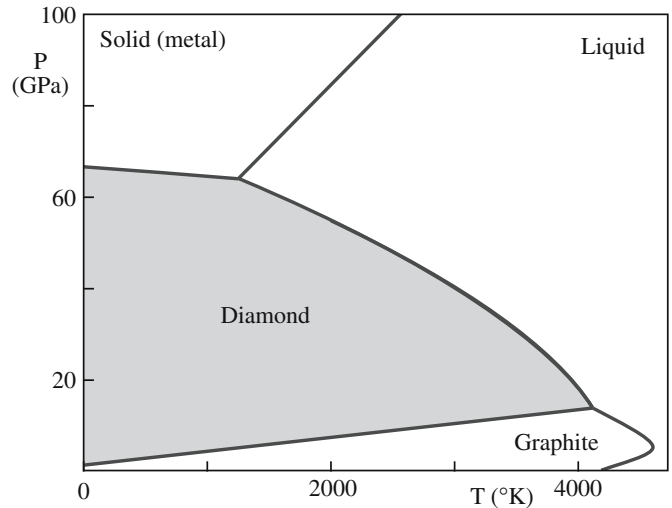


FIGURE 8.7 The C phase diagram.

phases are in equilibrium ( $X = 2$  and  $F = 1$ ). If we vary  $T$ , then  $P$  must vary so that we stay on the line. This diagram is a simplification of what we know now since there are many (11 or 12) other known crystalline forms of ice. The form that occurs in nature is called ice Ih (a hexagonal form) and has a density of  $0.931 \text{ g/cm}^3$  (water is  $1.00 \text{ g/cm}^3$ ; hence the iceberg phenomenon). The other forms exist at either lower values of  $T$  or higher values of  $P$  than shown in Figure 8.6. (We have kept this pressure in atm because the most important equilibrium occurs at 1 atm.)

Example 2: Carbon: One component (Figure 8.7). This is a classic example of an element with three solid phases. We often remind owners that diamonds are only metastable, but fortunately the kinetics of the phase transformation are very slow. Notice where we live—in a dot at the bottom left corner.

Example 3:  $\text{SiO}_2$ : One component (Figure 8.8). Silica is not only one of the most important ceramics, but its

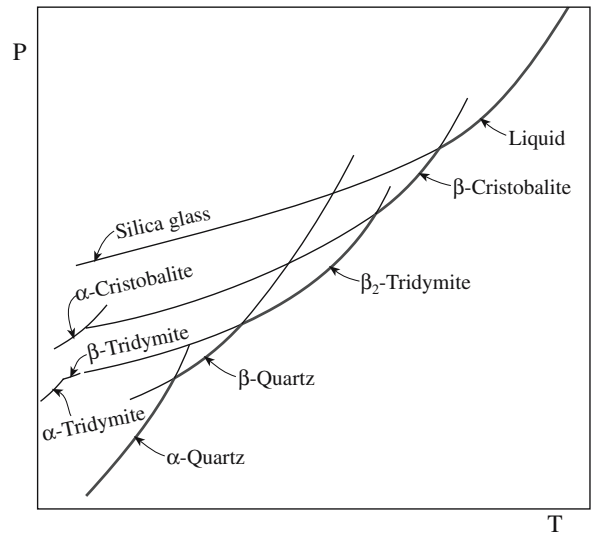


FIGURE 8.8 The  $\text{SiO}_2$  phase diagram.

phase diagram is also very interesting. Remember, the composition is constant. This schematic diagram emphasizes both the relationship between the glass and the liquid and the fact that the glass is the high-pressure phase; the glass is denser than any of the crystalline forms (similar to ice). The phase rules always apply.

## 8.6 TWO COMPONENTS ( $C = 2$ )

Binary phase diagrams are very important for ceramics. The two most important cases for ceramics are the combination of a metal plus oxygen and the combination of two oxides. A model two-component system is shown in Figure 8.9 where we are now using the third dimension to display the data.

If there is one phase ( $X = 1$ ) as at B, then the three variables are pressure, temperature, and one other, for example, the composition ( $x/y$  ratio).

If there are two phases present ( $X = 2$ ) such as the liquid and one solid phase at A, then  $F = 2$ . If, for example, we fix  $P$ , we are free to vary  $T$  and move along the liquid/solid phase boundary (a surface).

The special feature is that we have introduced surfaces into the phase diagram. In ceramic materials, the gas phase may be very important. This is where ceramics are particularly different from metals: oxygen (or nitrogen or water vapor and

### HUME-ROTHERY RULES FOR COMPLETE SOLID SOLUBILITY

- Same crystal structure
- Equal valence
- Ionic radius within  $\pm 15\%$
- No chemical reactivity

If we have two oxides we need consider only the sizes and valences of the cations.

hence hydrogen) may be a component of the system. The gas phase is not important if the valence of the cations is fixed and the total pressure,  $P$ , is fixed at 1 atm. We will consider materials with variable valence in Section 8.8.

Example 1: NiO/CoO: Two components and  $P$  fixed (Figure 8.10). The special feature about this diagram is that both oxides have a rocksalt structure. Pauling's rules tell us not to be surprised that they are fully interchangeable. However, it is reported that there is a two-phase region at low temperatures. Notice three points:

- At the high temperatures, the diagram contains only dashed lines—intelligent guesses.
- The two-phase region occurs where kinetics are quite slow.
- The composition is given as a mole fraction.

This is a case in which you start with “the book” and then go back to the original reference to learn how the  $pO_2$  was controlled, how the two phases were identified, etc.

Example 2: MgO/CaO:

Two components and  $P$  fixed (Figure 8.11). This diagram is a classic eutectic even though CaO and MgO both adopt the rocksalt structure. Because the sizes of the two cations differ by more than 15%, solid solubility is limited.

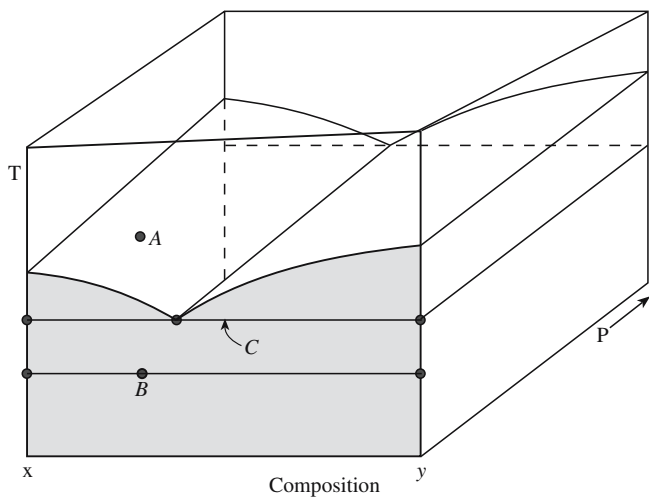


FIGURE 8.9 A model binary phase diagram showing  $T$ ,  $P$ , and composition as variables.

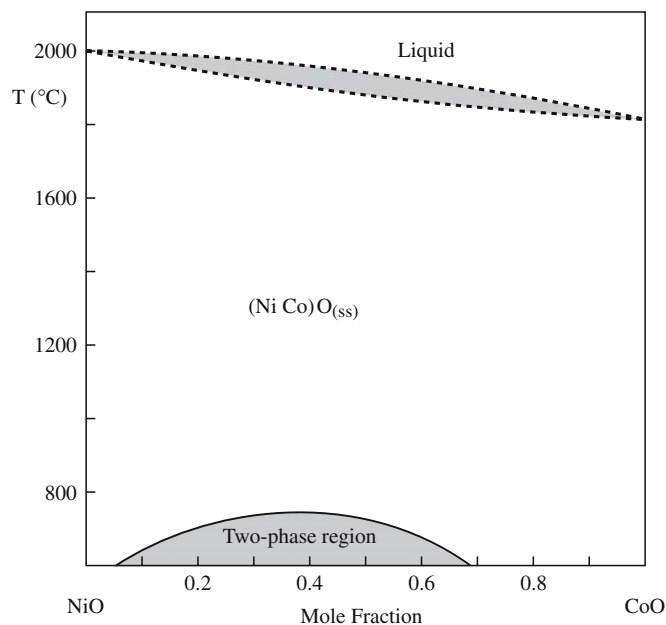


FIGURE 8.10 The NiO–CoO phase diagram.

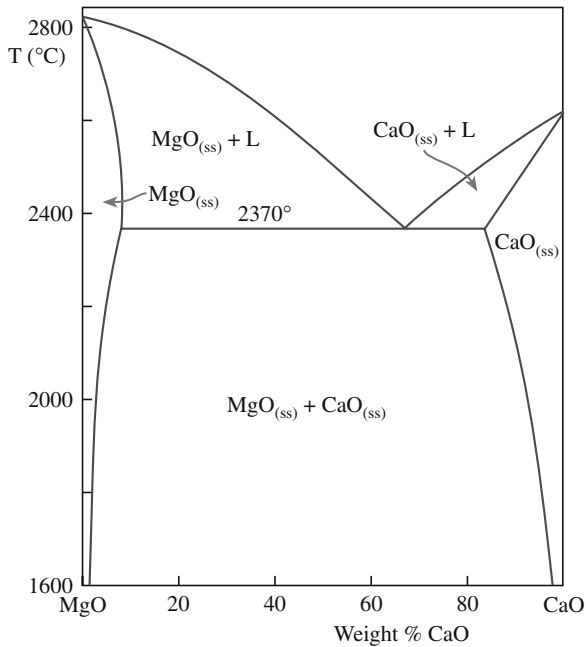


FIGURE 8.11 The MgO–CaO phase diagram.

Example 3: MgO/MgAl<sub>2</sub>O<sub>4</sub>/Al<sub>2</sub>O<sub>3</sub>: Two components and *P* fixed (Figure 8.12). This is a particularly important, but relatively simple, system in ceramics. It involves three widely used materials, which are also archetypical structures. We can choose the two components to be MgO and Al<sub>2</sub>O<sub>3</sub>. Then in the one-phase region we have one variable in addition to *P* and *T*. In the two-phase region we can vary *T* or the MgO:Al<sub>2</sub>O<sub>3</sub> ratio, but not independently. Notice that the composition is given in weight percent, which is not too bad for this system but really distorts the related MgO/Cr<sub>2</sub>O<sub>3</sub> and NiO/Al<sub>2</sub>O<sub>3</sub> systems. The spinel phase field is already quite wide at 1600°C and becomes wider at high temperatures, especially toward the Al<sub>2</sub>O<sub>3</sub>-rich

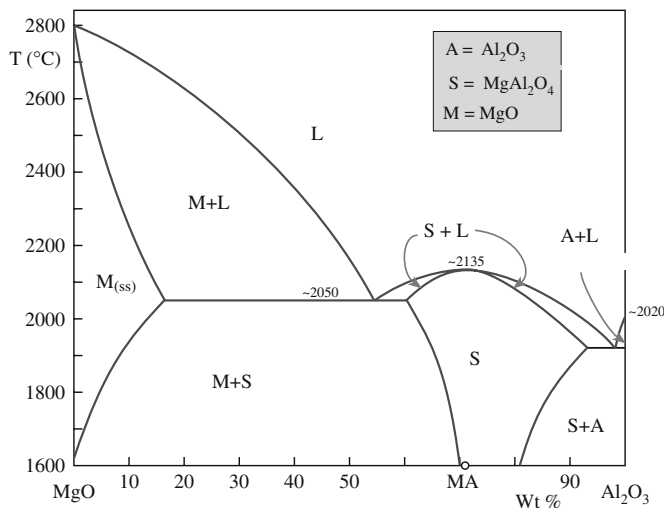


FIGURE 8.12 The MgO–Al<sub>2</sub>O<sub>3</sub> phase diagram.

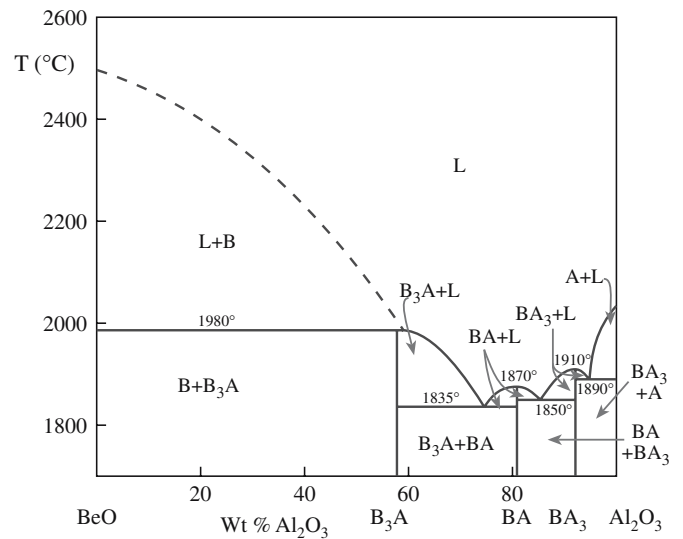


FIGURE 8.13 The BeO–Al<sub>2</sub>O<sub>3</sub> phase diagram.

side. We can grow two eutectic structures; one essentially contains pure Al<sub>2</sub>O<sub>3</sub>.

Example 4: BeO/Al<sub>2</sub>O<sub>3</sub>: Two components and *P* fixed (Figure 8.13). Notice that all the phases can be regarded as combinations of BeO and Al<sub>2</sub>O<sub>3</sub>, so we can denote them as B<sub>3</sub>A, BA, and BA<sub>3</sub>. From a chemical point of view, the system looks quite similar to MgO/Al<sub>2</sub>O<sub>3</sub>, but clearly it is very different; three separate eutectics are shown; none of the compounds has the spinel structure. BeAl<sub>2</sub>O<sub>4</sub> is the mineral chrysoberyl and has a structure similar to olivine, which is not unrelated to spinel.

Example 5: MgO/TiO<sub>2</sub>: Two components and *P* fixed (Figure 8.14). This system is interesting because of the

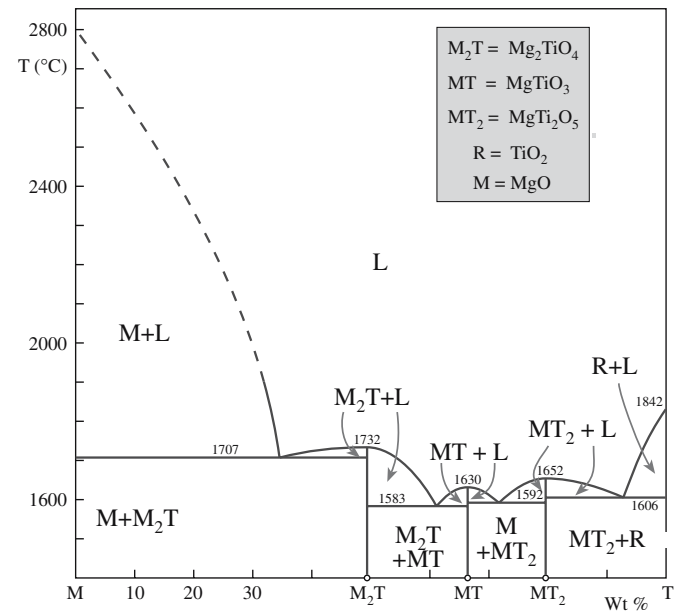
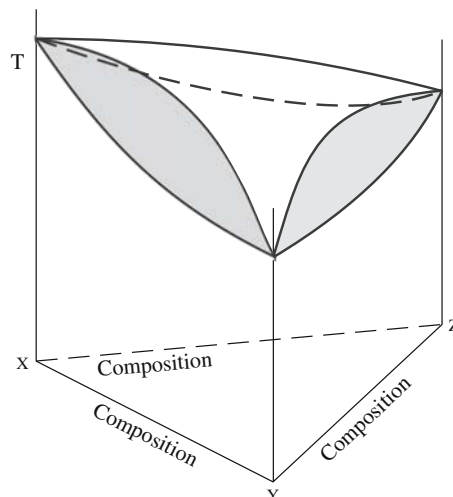
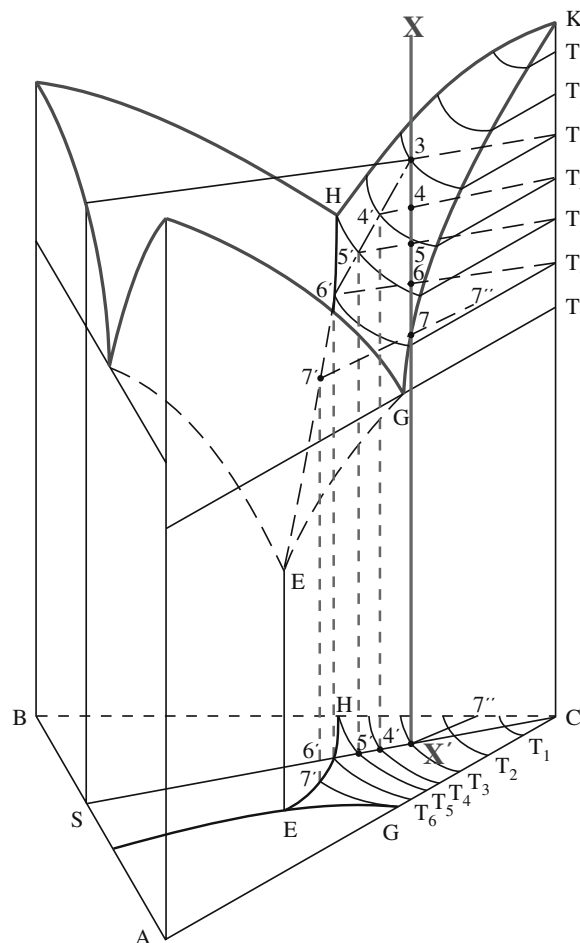


FIGURE 8.14 The MgO–TiO<sub>2</sub> phase diagram.

occurrence of four different eutectics. Such eutectics in this and other systems have been used to prepare some interesting two-phase materials. For example, when a liquid with composition in the MgO-rich region is cooled from the eutectic temperature at 1707°C it will produce a material that consists of alternating lamellae of nearly pure MgO and Mg<sub>2</sub>TiO<sub>4</sub>. Other systems show different structures, which are determined in part by the interfacial energies. Of course, interfacial energies are usually not considered in the analysis of phase diagrams.



(A)



(B)

**FIGURE 8.15** (a) A model ternary phase diagram for a system showing three solid solutions. (b) A model ternary phase diagram for a system showing three eutectics.

## 8.7 THREE AND MORE COMPONENTS

When three components (ternary systems;  $C = 3$ ) are present the phase diagrams become more difficult to draw because we then have  $F + X = 5$ . If the pressure is fixed then we have four variables. We need one axis for each component and one for the temperature, say, so we draw the compositions on a triangle and plot  $T$  as the vertical coordinate as shown in Figure 8.15a. The base triangle is called the Gibbs triangle. The example shown in Figure 8.15a corresponds to the case in which three oxides form solid solutions (extending the NiO/CoO example). The example shown in Figure 8.15b is the case of three simple binaries each with a single eutectic (extending the MgO/CaO example). Figure 8.15b is worth some effort to understand. The lines of constant temperature at the solid/liquid phase boundary are projected onto the base of the Gibbs triangle. The location of each of the three eutectics is also projected and will correspond to an abrupt change in the curvature of the constant-temperature contour. The three eutectics then meet at a “grand eutectic” at E. For sufficiently slow cooling, E will correspond to the ultimate eutectic temperature—below  $T_E$  the sample is solid.

In the materials that are often most important, the diagrams are more complicated. The phase diagram books then often show them as projected triangles as in Figures 8.16–8.18.

**Example 1:** MgO/Al<sub>2</sub>O<sub>3</sub>/SiO<sub>2</sub>: Three components and  $P$  fixed (Figure 8.16). Notice that there are perhaps three locations for E. This diagram contains several really important ceramics. We have already examined one of the binary diagrams included here (MgO/Al<sub>2</sub>O<sub>3</sub>) and will examine another below (MgO/SiO<sub>2</sub>). Diagrams like this have difficulty in showing what is happening at temperatures other than the liquidus.

**Example 2:** CaO/Al<sub>2</sub>O<sub>3</sub>/SiO<sub>2</sub>: Three components and  $P$  fixed (Figure 8.17). Figure 8.17 illustrates the extension of the use of abbreviations to three components. It also illustrates how the eutectics can be combined with a set of tie lines. The CA<sub>*n*</sub> ceramics are found in high-alumina cements. The phases are all shown as

being crystalline. Notice that CS is close to the midpoint, but that AS and CA are closer to Al<sub>2</sub>O<sub>3</sub>.

**Example 3:** Na<sub>2</sub>O/CaO/SiO<sub>2</sub>: Three components and  $P$  fixed (Figure 8.18). This system is particularly interesting because of its relevance to soda-lime glass

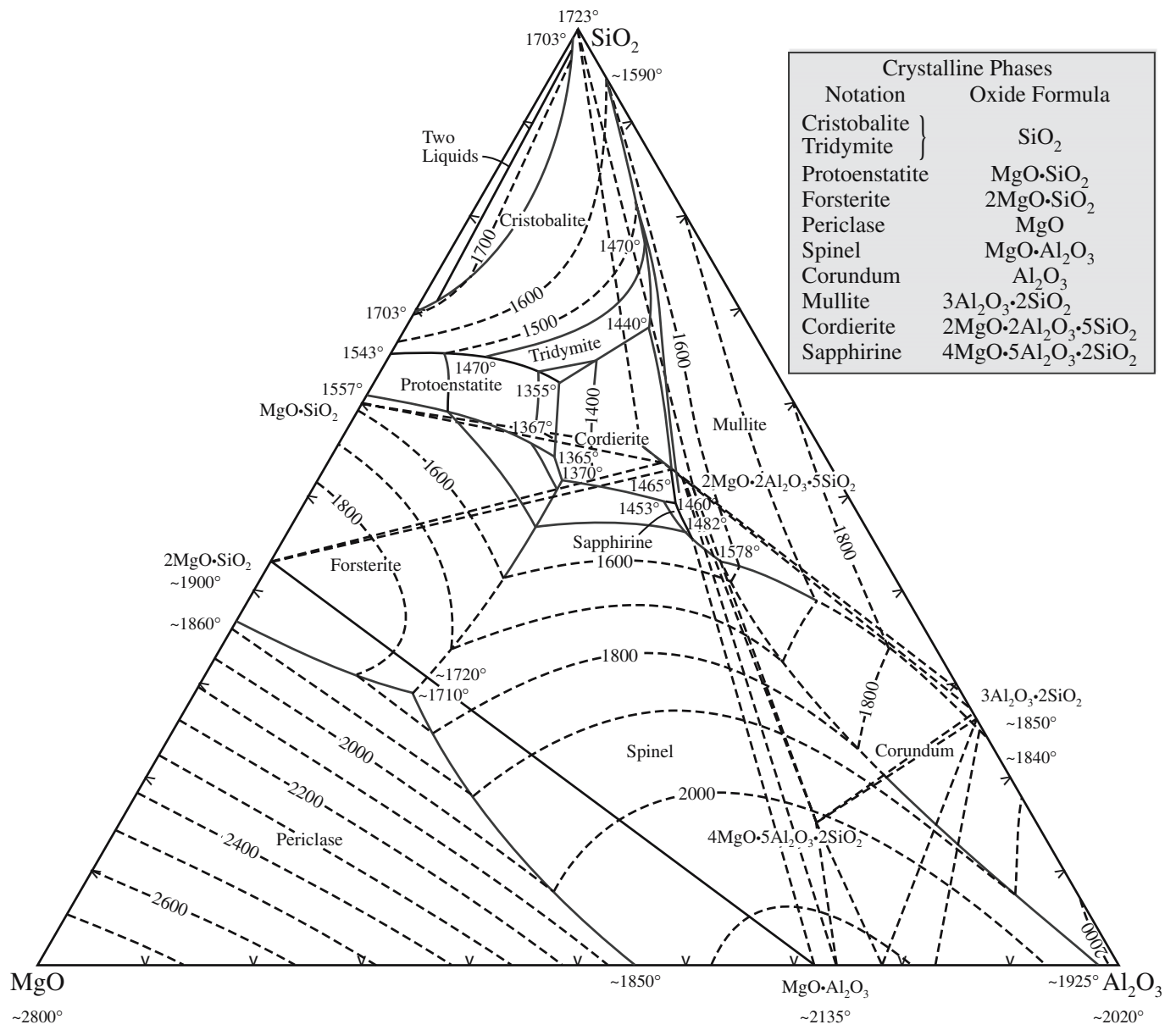


FIGURE 8.16 The MgO–Al<sub>2</sub>O<sub>3</sub>–SiO<sub>2</sub> phase diagram.

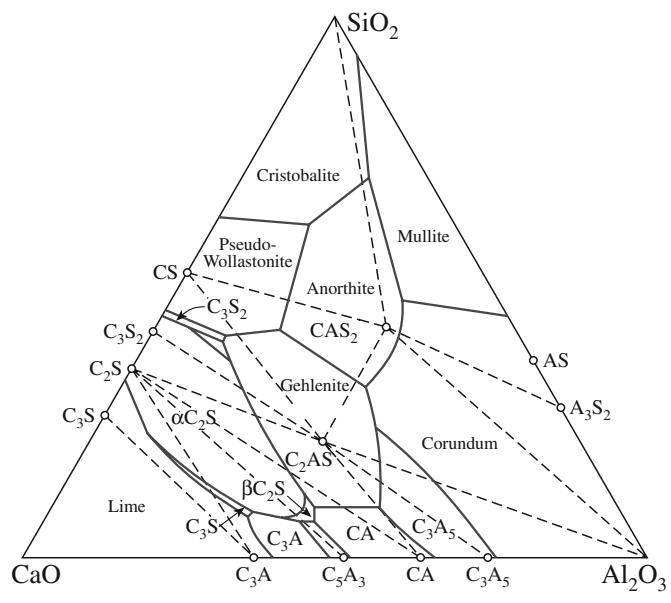


FIGURE 8.17 The CaO–SiO<sub>2</sub>–Al<sub>2</sub>O<sub>3</sub> phase diagram.

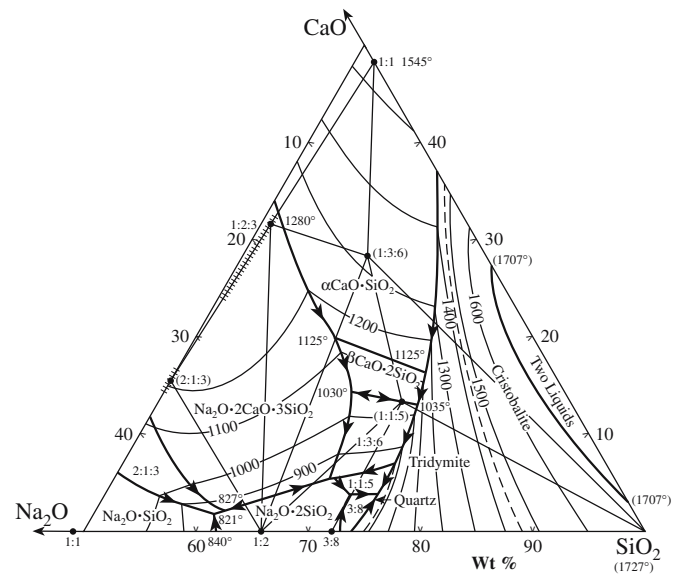


FIGURE 8.18 The Na<sub>2</sub>O–CaO–SiO<sub>2</sub> phase diagram.

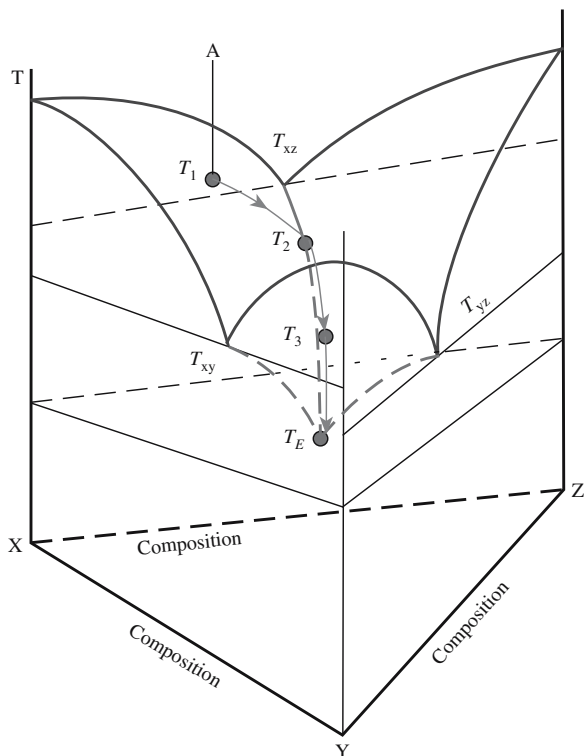


FIGURE 8.19 Illustration of a cooling path in a ternary system.

formation. Because of this interest, the diagram has been limited to the silica-rich corner of the Gibbs triangle.

Each of these diagrams shows the contours of the solid/liquid boundary. It is now a little more difficult to envision what occurs as we lower the temperature of the liquid phase. The basic ideas are the same as for the two-component systems as shown in Figure 8.19. The cooling path follows the steepest descent on the liquidus until, in this case, it reaches  $T_E$ , at which point the whole sample is solid and kinetics become the controlling factor.

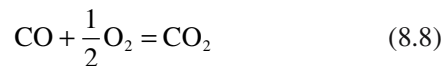
## 8.8 COMPOSITION WITH VARIABLE OXYGEN PARTIAL PRESSURE

The gas phase, particularly the oxygen partial pressure,  $pO_2$ , is important when the valence of the cation can change.

In ceramics, we usually run experiments at 1 atm, but geologists are interested in much higher pressures, and hot pressing is an established commercial method for processing ceramics.

There are two ways to control the  $pO_2$ . Usually, we do not try to change or control the total pressure—we avoid vacuum systems whenever possible because they greatly

increase the expense. The approach used is to fix the  $pO_2$  using one of the following reactions:



If there is no solid present then we just have one phase, namely, the gas, and  $X + F = C + 2$  gives  $F = 3$ . So we can vary  $T$ ,  $P_{total}$ , and the composition ( $CO_2/CO$  ratio or  $H_2/H_2O$  ratio).

If there is a solid present (e.g., graphite or Ni) then we have just two variables (since we have two phases,  $X = 2$ ), which will fix the system. If Ni is present, for example, then essentially the Ni/NiO equilibrium sets the  $pO_2$ . The same occurs if Fe is present.

We will spend some time discussing the Fe–O diagram shown in Figure 8.20; here gas is important. In the Fe–O phase diagram, we have two components. We can call them Fe and O or FeO and  $Fe_2O_3$  as we wish. The special feature in Figure 8.20 is the fact that usually the lines of constant  $pO_2$  are horizontal whereas in two-phase fields they are inclined to the horizontal. They are inclined when the phase field contains a single phase (wüstite or magnetite).

In the two condensed phases region (region W + M: wüstite plus magnetite) there are two condensed phases plus the gas ( $O_2$ ), so  $X = 3$ . There are two components ( $C = 2$ ; Fe and O), so we have only one degree of freedom: we can vary  $T$  or  $pO_2$ . So the oxygen isobars (lines of constant  $pO_2$ ) on the phase diagram must be horizontal.

In the wüstite phase (region W) there is one condensed phase plus the gas ( $O_2$ ), so  $X = 2$ . There are two components ( $C = 2$ ; Fe and O), so we have two degrees of freedom ( $F = 2$ ). The reason the isobars have the particular slope is that they must connect the appropriate isobars at each side of their phase field.

This is the special feature for ceramics, especially when processing ceramics with a variable-valence cation in air:  $pO_2$  is important.

The diagram in Figure 8.20b shows the Fe–O diagram as a function of oxygen activity, which is essentially the  $pO_2$ . This diagram shows what condensed phase is stable at

each combination of temperature and  $pO_2$ . Although this diagram does not show as much information as Figure 8.20a (because it does not show the composition of the condensed phase), it does emphasize one special feature: if we increase the temperature while keeping the  $pO_2$  constant, the oxidation state of the Fe ion decreases. In Figure 8.20b, the areas show situations in which only one phase is

### PRESSURE CONVERSION

- 1 Pa = 1 N m<sup>-2</sup> = 1 m<sup>-1</sup>·kg s<sup>-2</sup>
- 1 N = 1 m·kg s<sup>-2</sup>
- 1 bar = 0.1 MPa
- 1 kbar = 100 MPa
- 1 atm = 1.013 Pa
- 1 mm Hg = 1 torr = 0.1333 MPa

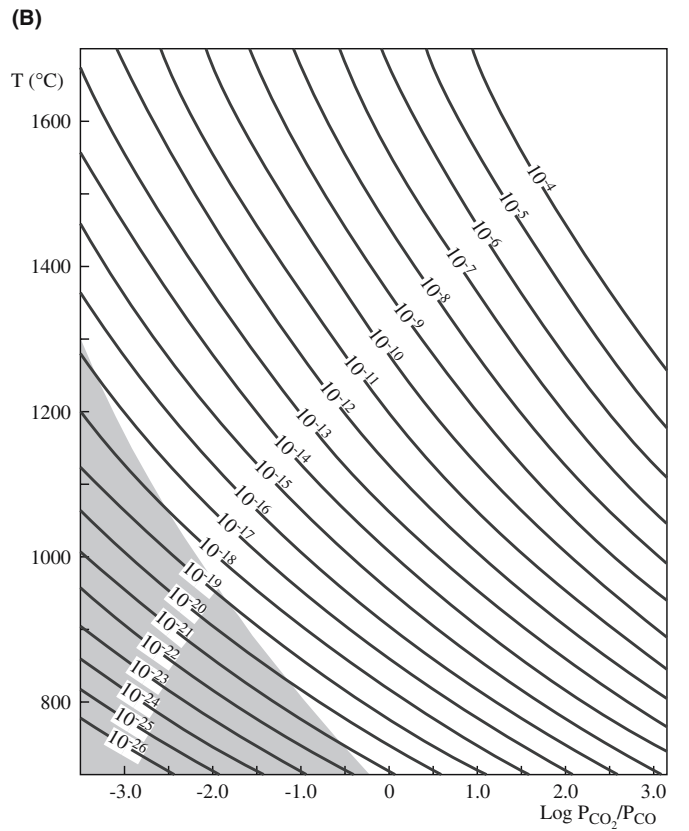
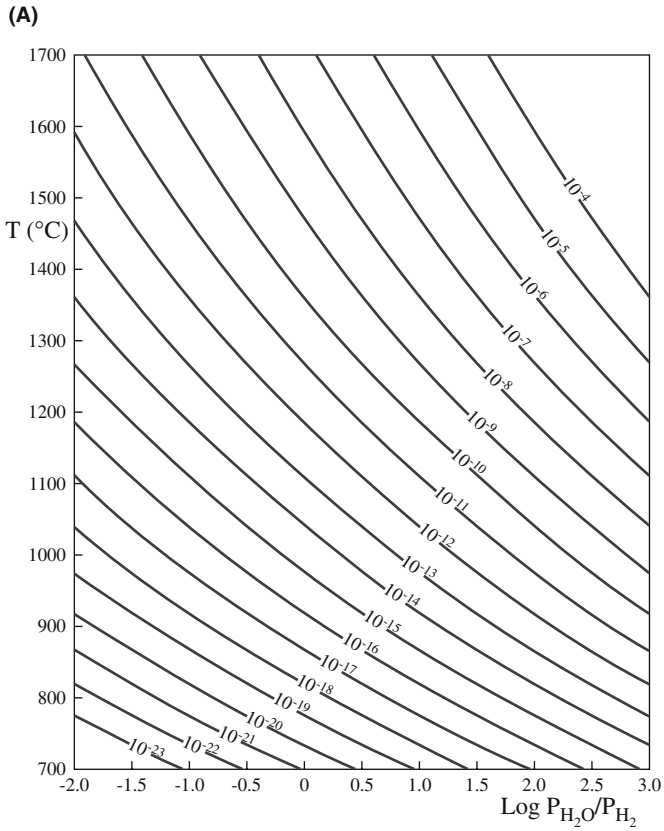
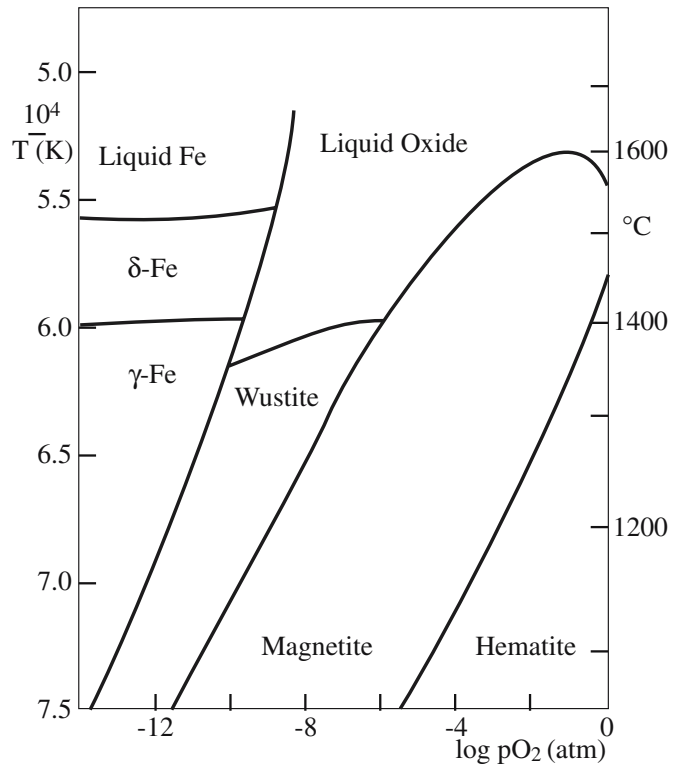
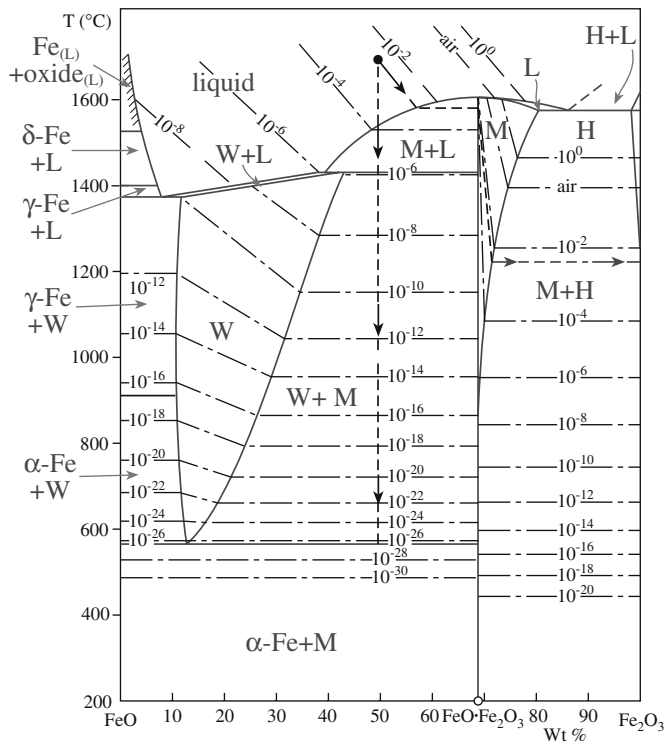


FIGURE 8.20 (a, b) The FeO–Fe<sub>2</sub>O<sub>3</sub> phase diagram; (c) the H–O system; (d) the C–O system.



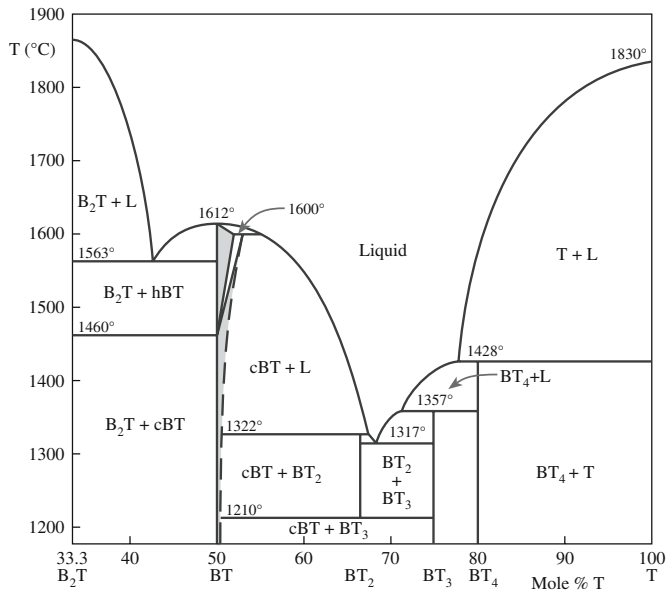


FIGURE 8.23 The BaTiO<sub>3</sub> phase diagram.

system (Figure 8.23). This diagram illustrates the concept of incongruent melting: there are actually three incongruently melting compounds. The diagram also shows that we cannot produce pure cubic BaTiO<sub>3</sub> by solidifying a liquid of that composition, which will be important when we discuss crystal growth later. Notice that all the compounds on this phase diagram are BT<sub>n</sub> (BT, BT<sub>4</sub>, etc.)

## 8.11 MISCIBILITY GAPS IN GLASS

Can glass be described by equilibrium phase diagrams? The question refers to the fact that glass is not itself in equilibrium. We can, however, describe some aspects of the glass microstructure in terms of phase diagrams, especially that of liquid immiscibility, which leads to the phenomenon of phase separation as illustrated in Figure 8.24.

The random-network model considers glasses as homogeneous. However, microscopic features on the scale of 3 nm to hundreds of nanometers can exist. These small features exist in a range of glasses and can result from a process of phase separation, in which a liquid that is homogeneous at high temperatures separates into two or more liquid phases on cooling.

Figure 8.25 shows the phase diagram for the BaO–SiO<sub>2</sub> system, which exhibits phase separation. The dome, shown by dashed lines because the system is metastable, is the key feature in a phase diagram in which phase separation occurs (a similar dome occurs for Al<sub>2</sub>O<sub>3</sub>/Cr<sub>2</sub>O<sub>3</sub>, so this dome is not peculiar to glass).

The microstructure of glasses in the system BaO–SiO<sub>2</sub> can be determined using transmission electron microscopy (TEM). We find the following:

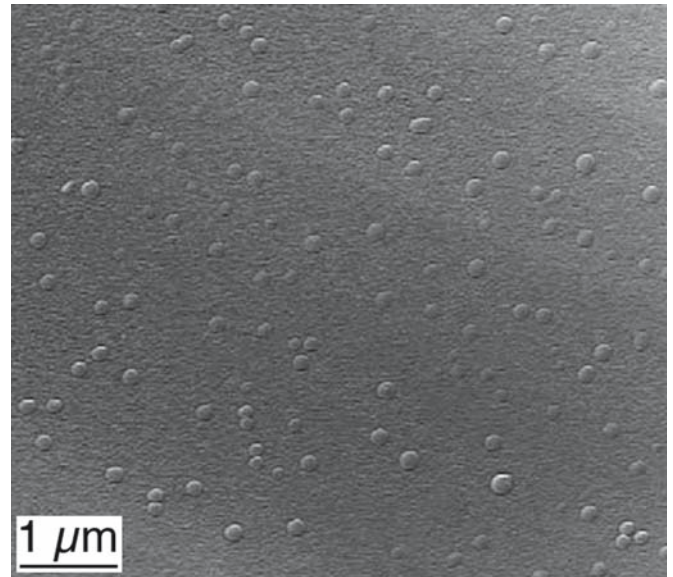


FIGURE 8.24 Image of small droplets of glass in a glass matrix. The composition of the glass is 16wt% CaO, 10wt% MgO, 14wt% Al<sub>2</sub>O<sub>3</sub>, and 60wt% SiO<sub>2</sub>.

- At the silica rich side of the miscibility gap there are discrete spherical particles of a BaO-rich phase embedded in a continuous matrix of an SiO<sub>2</sub>-rich phase.
- Near the center of the miscibility gap there is a three-dimensionally interconnected mixture of BaO and SiO<sub>2</sub> phases.

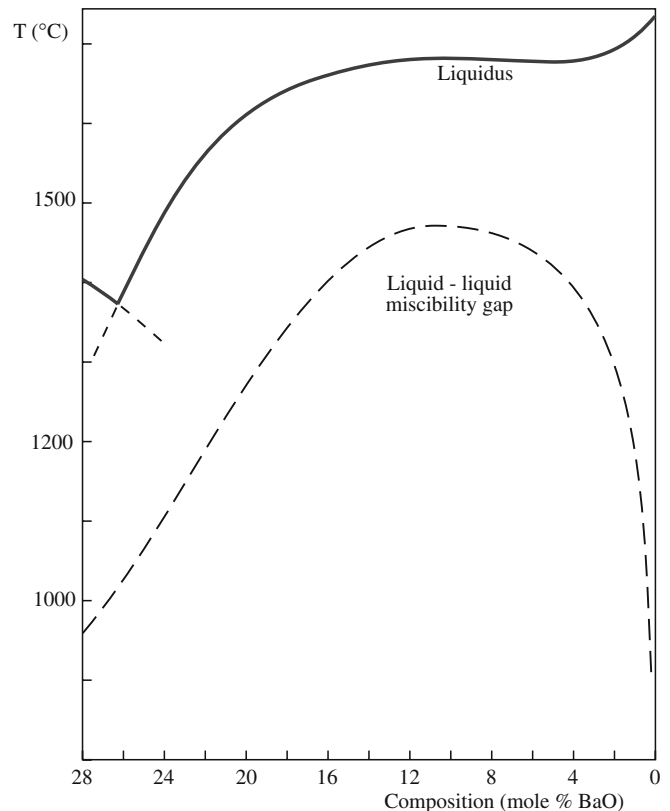
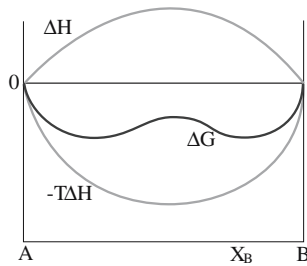


FIGURE 8.25 The silica-rich end of the BaO–SiO<sub>2</sub> phase diagram.



**FIGURE 8.26** Energy diagram for a hypothetical system in which unmixing occurs.

- At the BaO-rich side of the miscibility gap there are discrete spherical particles of an SiO<sub>2</sub>-rich phase embedded in a continuous matrix of a BaO-rich phase.

The B<sub>2</sub>O<sub>3</sub>–PbO system is another glass-forming system that shows a miscibility gap and phase separation.

The reason for phase separation of a liquid into two phases may be found by consideration of the thermodynamics of mixing. Figure 8.26 shows the three thermodynamic functions,  $\Delta G$ ,  $\Delta H$ , and  $\Delta S$ , plotted at temperature  $T$  as a function of composition.

The common tangent to the minima in the free-energy curve determines the composition of the two phases in the glass and the proportions of each are determined by the lever rule.

### GIBBS FREE ENERGY OF MIXING

For an ideal solution  $\Delta G_M$  is

$$\Delta G_M = RT(X_A \ln X_A + X_B \ln X_B)$$

and  $\Delta H_M = 0$ .

For nonideal solutions,  $\Delta H_M \neq 0$ .

Phase separation is important for some commercial glass formulations.

**Vycor Process:** Glass containing 75 wt% SiO<sub>2</sub>, 20 wt% B<sub>2</sub>O<sub>3</sub>, and 5 wt% Na<sub>2</sub>O melts at relatively low temperatures due to the high B<sub>2</sub>O<sub>3</sub> content. It can then be formed into desired shapes and heat treated in the range of 500–600°C so that the glass separates into two distinct phases, one consisting of almost pure SiO<sub>2</sub> and another rich in Na<sub>2</sub>O and B<sub>2</sub>O<sub>3</sub>. If this product is exposed to a suitable solvent at modest temperature, the sodium borate phase is leached out, leaving an SiO<sub>2</sub>-rich framework with a network of

pores that are ~4–15 nm in diameter. This porous glass can be subsequently compacted at ~1000°C to yield a transparent glass containing about 96 wt% SiO<sub>2</sub>. The advantage of this process is that we can form this silica-rich glass at relatively low tempera-

ture. It would not be feasible to shape 96% silica glass by conventional methods because of the very high temperatures required to decrease the viscosity of a high-silica glass.

**Pyrex:** Pyrex glass also belongs to the Na<sub>2</sub>O–B<sub>2</sub>O<sub>3</sub>–SiO<sub>2</sub>-system. It exhibits phase separation on a very fine scale, typically less than 5 nm. By controlling the cooling process, we develop a glass with a special microstructure and very useful properties. It is the inclusion of a soluble phase within an insoluble one that explains the chemical durability of Pyrex.

## CHAPTER SUMMARY

Phase diagrams are the key to understanding many aspects of ceramic processing. Whether we are interested in forming a material by a solid-state reaction or growing a single crystal by solidification of a melt, the first approach is to look up the appropriate phase diagram. Knowing where to find these diagrams (in the “books”) is almost as important as being able to interpret them. The basic principles are the same for ceramics as they are for metals. So our approach was to highlight some important aspects of phase diagrams as they relate to ceramics.

### PEOPLE IN HISTORY

Gibbs, Josiah Willard (1839–1903) was born in New Haven, Connecticut. He was educated at Yale University and was awarded his doctorate in 1863—the first doctorate of engineering to be conferred in the United States. He was appointed professor of mathematical physics in 1871 prior to having any publications. He published the first part of his very famous work *On the Equilibrium of Heterogeneous Substances* in 1876 and the second part in 1878. He published many other important papers in thermodynamics as well as other areas of physical science.

Hume-Rothery, William (1899–1968) founded the Department of Metallurgy (now the Department of Materials) at Oxford University in the mid-1950s. HR, as he was known at Oxford, was the author of many books on metallurgy. One of his books, *Electrons, Atoms, Metals, and Alloys*, is a dialogue between an older metallurgist and a younger scientist.

Le Chatelier, Henry (1850–1936) is known for his principle and for inventing the optical pyrometer in 1892.

## GENERAL REFERENCES

Bergeron, C.G. and Risbud, S.H. (1984) *Introduction to Phase Equilibria in Ceramics*, The American Ceramic Society, Westerville, OH. This should be available in every ceramics laboratory.  
DeHoff, R.T. (2006) *Thermodynamics in Materials Science*, 2nd edition, CRC, Boca Raton, FL.  
Gaskell, D.R. (2003) *Introduction to the Thermodynamics of Materials*, 4th edition, Taylor & Francis, New York.

Hummel F.A. (1984) *Phase Equilibria in Ceramic Systems*, Marcel Dekker, New York.

McHale, A.E. (1998) *Phase Diagrams and Ceramic Processes*, Chapman & Hall, New York.

Muan, A. and Osborn, E.F. (1965) *Phase Equilibria among Oxides in Steelmaking*, Addison-Wesley Publishing Co., Reading, MA. Reference for experimental determination of phase diagrams in ceramics. Inspirational with very helpful commentary; a “must see” text.

*Phase Diagrams for Ceramists, Vols. I–VIII*, The American Ceramic Society, Columbus, OH:

I (1964) edited by E.M. Levin, C.R. Robbins, and H.F. McMurdie

II (1969) edited by E.M. Levin, C.R. Robbins, and H.F. McMurdie

III (1973) edited by E.M. Levin and H.F. McMurdie

IV (1981) edited by R.S. Roth, T. Negas, and L.P. Cook

V (1983) edited by R.S. Roth, T. Negas, and L.P. Cook

VI (1987) edited by R.S. Roth, J.R. Dennis, and H.F. McMurdie

Volumes I–VI include mostly oxide and metal + oxide systems.

VII (1989) edited by L.P. Cook and H.F. McMurdie (halide systems, many calculated diagrams with methods discussed)

VIII (1990) edited by B.O. Mysen (geological, high pressure, and hydrothermal systems)

Under a new series title, but continuous numbering, *Phase Equilibria Diagrams, Vols. IX–XII*:

IX (1992) “Semiconductors and Chalcogenides,” edited by G.B. Stringfellow

X (1994) “Borides, Carbides, and Nitrides,” edited by A.E. McHale

XI (1995) “Oxides,” edited by R.S. Roth

XII (1996) “Oxides,” edited by A.E. McHale and R.S. Roth

The books are available on CD-ROM from [www.esm-software.com/pd-ceramists](http://www.esm-software.com/pd-ceramists) but are too costly for most individuals.

Also a part of this series are *Phase Equilibrium Diagrams, Annuals '91, '92, and '93*, edited by A.E. McHale (these annuals contain a number of complex oxide systems), and *Phase Diagrams for High  $T_c$  Superconductors*, edited by J.D. Whitler and R.S. Roth (1991).

Ragone, D.V. (1995) *Thermodynamics of Materials*, Volume I, Wiley, New York.

Swalin, R.A. (1972) *Thermodynamics of Solids*, 2nd edition, Wiley, New York.

## WWW

<http://thayer.dartmouth.edu/%7Eicelab/> The site of the ice laboratory at Dartmouth.

<http://www.ceramics.nist.gov/webbook/glossary/ped/glossary.htm> NIST’s site for phase equilibria of ceramics.

## SPECIFIC REFERENCES

CALPHAD [computer file], Elsevier, New York. Available in many university libraries on line.

Ellingham, H.J.T. (1944) “Reducibility of oxides and sulfides in metallurgical processes,” *J. Soc. Chem. Ind. (London)* **63**, 125.

Hazen, R.M. (1999) *The Diamond Makers*, Cambridge University Press, Cambridge. Attaining the high pressures.

Richardson, F.D. and Jeffes, J.H.E. (1948) “The thermodynamics of substances of interest in iron and steel making from 0°C to 2400°C,” *J. Iron Steel Inst. (London)* **160**, 261.

Saunders, N. and Miodownik, A.P. (1988) *CALPHAD (Calculation of Phase Diagrams): A Comprehensive Guide*, Pergamon, Oxford.

Torres, F.C. and Alarcón, J. (2004) “Mechanism of crystallization of pyroxene-based glass-ceramic glazes,” *J. Non-Cryst. Sol.* **347**, 45.

## EXERCISES

- 8.1. The iron–iron carbide phase diagram is probably the most important of all binary phase diagrams. Why is the diagram not a true equilibrium diagram? Does it matter?
- 8.2. Explain what we mean by the set of equations  $\mu_1^a = \mu_1^b = \dots = \mu_1^c$ . What is the significance of this expression?

- 8.3 The maximum operating temperature of high-temperature X-ray diffraction is 2500°C in vacuum but only 1700°C in air. Why the big difference? What, if any, effect would the lower operating temperature in air have on the determination of phase diagrams?
- 8.4 The  $\text{UO}_2\text{-BeO}$  system shown in Figure 8.3 does not show any solid solution formation. Would you expect it to?
- 8.5 With reference to the phase diagram for water (Figure 8.6), explain (a) how the boiling point of water would change if you were to climb to the top of a mountain and (b) why ice-skating is possible.
- 8.6 Using Figure 8.7 determine the necessary conditions for direct conversion of graphite to diamond.
- 8.7 Using Figure 8.8 indicate all the triple points in the  $\text{SiO}_2$  system.
- 8.9 Describe fully what happens when you cool down a melt of 40 mol% NiO–60 mol% MgO. Give the compositions of the phases and their relative amounts for at least three temperatures in the two-phase field.
- 8.10 Describe the phases that you expect to form as a liquid of composition  $\text{BaTiO}_3$  is cooled down to room temperature. Given the statement we make in Section 8.10 about the growth of single crystals of cubic  $\text{BaTiO}_3$ , what factors besides thermodynamics determine our ability to grow single crystals?